Program Digest, 2019 IEEE International Ultrasonics Symposium (IUS)
Glasgow, Scotland, October 6-9, 2019

Optimization of virtual sources distribution in 3D echography

Goulven Le Moign*†, Nicolas Quaegebeur†, Patrice Masson†, Olivier Basset*, Marc Robini* and Hervé Liebgott*

* CREATIS, Univ.Lyon, INSA-Lyon, UCBL1, CNRS UMR 5220, Inserm U1206, UJM-Saint Etienne.
69100, Villeurbanne, France
† GAUS, Dept. Mechanical Engineering, Université de Sherbrooke, Sherbrooke, QC, Canada J1K 2R1

e-mail: goulven.le.moign@usherbrooke.ca

***Abstract*—Coherent compounding may be applied with diverging waves on 2D ultrasound probes to overcome the problem of small aperture probe and meet the requirement for high frame rate 3D imaging, as in transthoracic echography for example. Deterministic distributions of the virtual sources are often used in practice. The compromise between contrast and resolution has to be managed according to the application, and this will affect the distribution of the virtual sources. This study proposes to use a multi-objective optimization genetic algorithm to allow some freedom in the management of this compromise. The solutions obtained are compared to the case of a regular and a spiral distribution of sources. The results show that virtual sources distribution can produce images with the emphasis on either contrast or lateral resolution, and validate observations already reported in the literature.**

***Index Terms*—3D echography, 2D probe, coherent compounding, diverging waves, multi-objective optimization genetic algorithm**

I. Introduction

Three-dimensional (3D) ultrafast echography with two-dimensional (2D) probes allows tracking the dynamics of organs, like the heart [1,2], and allows obtaining further information, which helps the clinician doing a better medical diagnosis. However, 3D ultrafast echography remains a challenging application because of the complexity to maintain a high frame rate while guaranteeing a sufficient image quality for post-processing algorithms. Coherent Compounding (CC) [2,3] overcomes that difficulty, such that it is currently a popular transmitting strategy in ultrafast echography. The principle is to transmit several unfocused waves to reconstruct a high quality image. The unfocused waves can be either plane or diverging. When generating Diverging Waves (DW), each wave is associated with the position of a Virtual Source (VS).

Up to now, regular distribution of the VS is often used in practice; however, the resulting image can be enhanced in terms of resolution or contrast by optimizing the VS positions.

This study consists in finding optimized distribution of the VS as a function of the desired quality metric: lateral resolution or contrast. A multi-objective optimization framework has thus been developed in order to put the emphasis on either contrast or lateral resolution for images of 3D Point Spread Function (PSF).

II. Method

A. Imaging configuration

A 32×32 elements probe is simulated using the Field II software [4,5] in MATLAB [6]. The pitch is fixed at $\frac{\lambda}{2}$ where $\lambda = \frac{c_p}{f_c}$ is the wavelength, c_p = 1540 m/s is the compressional wave velocity, and f_c = 3 MHz is the central frequency of the elements. A single point-like scatterer is located at (x,y,z) = (0,0,40) mm, where x and y are the two lateral dimensions and z the depth, in order to obtain a 3D PSF for further processing. The center of the probe is assimilated to the origin of the coordinate system. The 3D grid of the reconstructed images is (x,y,z) = $20 \times 20 \times 10$ mm with a step of $\frac{\lambda}{2}$ in each , resulting in $78 \times 78 \times 39$ pixels.

For cardiac imaging, DW are commonly used because a large Region Of Interest (ROI) is required ($\sim$ 8 cm in the lateral direction) and the aperture of the probe has to be small enough ($\sim$ 1 cm) to fit the intercostal space. The VS are located behind the probe. Theses DW are associated with the position of a VS, a point-like acoustic source placed behind the probe plane when the ROI is in front of it.

A standard Delay-and-Sum beamforming is then used to reconstruct the images for each DW. No apodization is applied in transmission and reception. Twenty-five DW are transmitted to reconstruct an image with the CC method, *i.e.* by adding coherently all the images in order to obtain the final image, so that resolution, contrast and *Signal-to-Noise Ratio* (SNR) can be improved. This method allows choosing a compromise between image quality and frame rate, or fixing the frame rate under the constraint that the frame rate has to match tracking algorithms. The quality is comparable to a synthetic aperture imaging and conventional echography when a large number of VS (> 25) is used. However, the resulting image quality is strongly dependent on the position and number of VS, such that these parameters have to be optimized.

B. Cost functions

Two cost functions are extracted from the PSF to quantify the quality of the reconstructed images and derive an optimization framework: one for the lateral resolution and a another one for the contrast. The inputs of these cost functions are the 2D spherical coordinates (θ, ϕ). The distance between the VS and the center of the probe (Fig. 1) is constant for all VS in order to reduce the number of input arguments. This distance is then fixed at 40 mm, as used in preceding work [7].

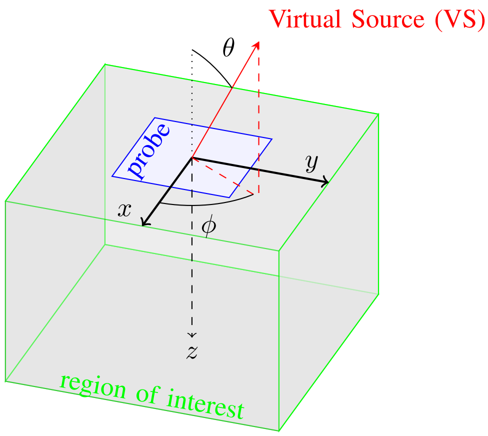

Fig. 1: Position of the probe, the ROI and the virtual sources

The maximum elevation angle θ which can be reached out is fixed at 20°, in order to reduce computation time and increase convergence rate, and because a high θ produces more artefacts on the images due to secondary lobes.

For the resolution cost function, all pixels above -6 dB are projected along the z-axis in order to focus on the lateral spread in 2D (Fig. 2); the area of that projection is measured and then the average diameter is calculated.

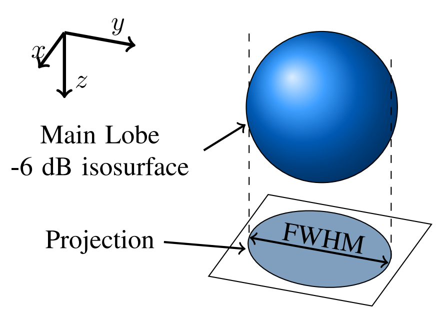

Fig. 2: Lateral resolution (FWHM) measurement by projection

By doing so, this 1-D measurement corresponds to the standard Full Width at Half Maximum (FWHM) measurement.

For the contrast, the Maximum Side-lobe Level (MSL) is measured using an online toolbox [8] in order to minimize the side-lobe level, which is related to contrast. Fig. 3 the standard 1D MSL measurement :

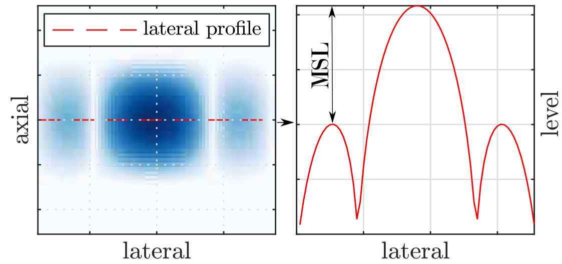

Fig. 3: Standard 1D Main-to-Side-lobe Level (MSL) measurement

C. Multi-objective Optimization

As there is a compromise to achieve between contrast and resolution [9] that will depend on the application, a non-dominated front approach [10], that is, a set of solutions that best represents the Pareto front [11,12], has been chosen to perform a multi-objective optimization. In that way, a single run of optimization generates a set of trade-offs between contrast and resolution. Evolutionary Algorithms (EA), such as Genetic Algorithm (GA) [13,14] and Particle Swarm Optimization (PSO) [15], are suitable to handle multi-objective optimization. Different tools for Multi-objective Optimization Evolutionary Algorithms (MOEA) have been proposed [10]–[12]. The `gamultiobj` toolbox available in MATLAB [6], based on fast Non-dominated Sorting Genetic Algorithm (NSGA-II) [16], has been used to perform the optimizations. The population here is set to 1000 individuals (solutions), with a 40 % cross-over fraction and a 4 individuals tournament selection.

III. Results

The results are presented over the objective space, which is the space representing all the costs (MSL and FWHM) for each solution. It helps evaluating this optimization performance (position and spread of the non-dominated front), and interpreting results like the choice of the proper compromise to be made. The optimization ends after 250 generations, and all the non-dominated solution have been saved (25) to produce a non-dominated front. Two additional deterministic configurations are added as a comparison: a regular (a) and a spiral (b) distribution represented in Fig. 4, originating from [7,17].

Fig. 5 presents the performance in the objective space of the stated solutions, in terms of MSL and FWHM.

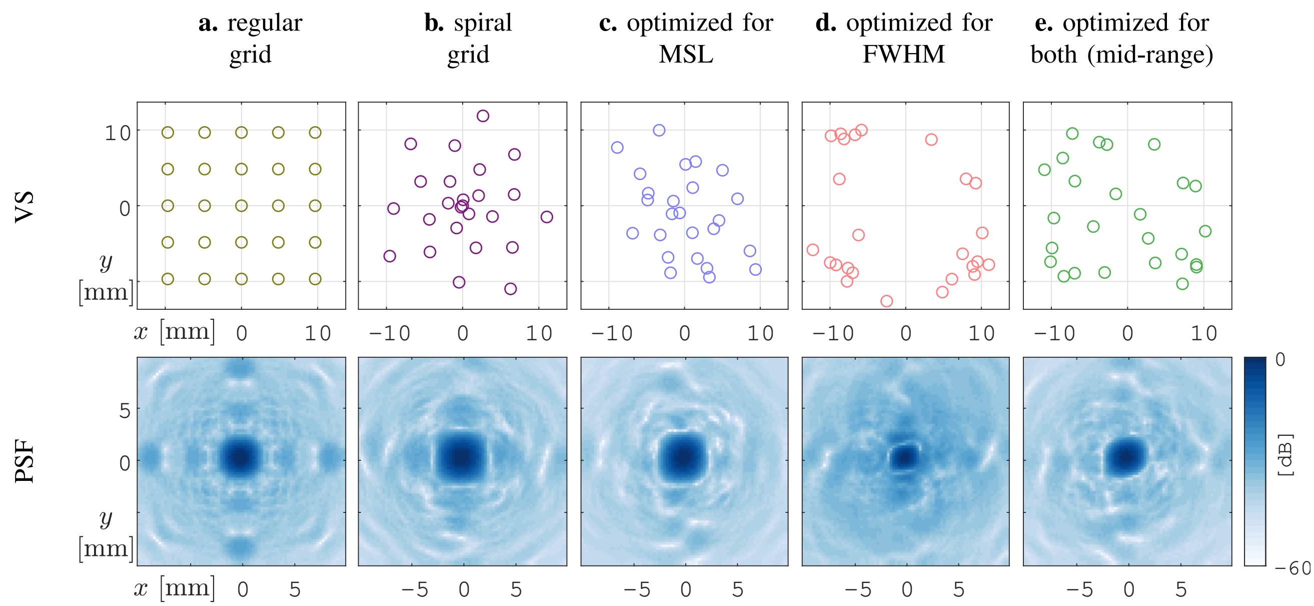

MSL	-24.9 dB	-26.3 dB	-32.2 dB	-21.4 dB	-29.3 dB
FWHM	1.92 mm	2.28 mm	2.11 mm	1.25 mm	1.65 mm

Fig. 4: VS distribution and PSF for 5 configurations: regular (**a.**), spiral (**b.**), optimized for MSL (**c.**), optimized for FWHM (**d.**), and optimized for both MSL and FWHM (mid-range, **e.**)

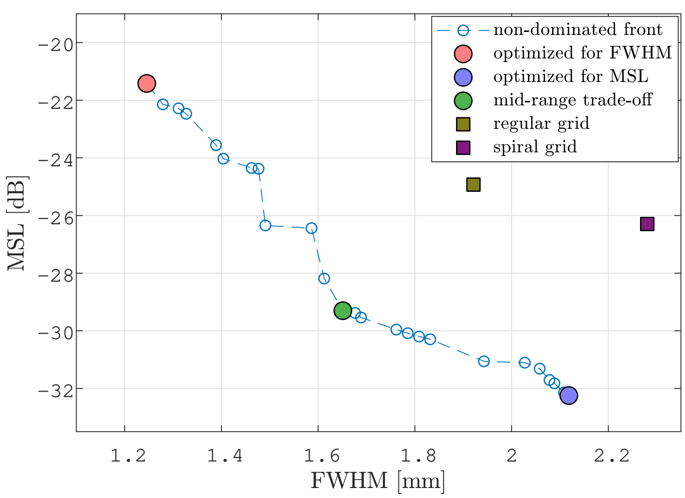

Fig. 5: Solutions in the objective space (MSL and FWHM): non-dominated front obtained after the multi-optimization of the VS, regular and spiral distributions

The non-dominated front shows solutions between 1.25 and 2.11 mm for the FWHM measurement and from -21.4 to -32.2 dB for the MSL measurement. The non-dominated front helps revealing that both regular grid and spiral distribution used classically are not optimal solutions, with respect to these quality assessments.

Three specific solutions are extracted from the non-dominated front: the best in FWHM, the best in MSL and a mid-range trade-off. Their VS distributions are displayed in Fig. 4 with the resulting xy images computed at scatterer's depth.

The regular distribution (a) shows better FWHM than the spiral (b) (from 2.28 mm to 1.92 mm) whereas the MSL is better on the spiral (-26.3 dB) than the regular distribution (-24.9 dB). Optimizing the FWHM helps enhancing the lateral resolution (c) on the displayed PSF and likewise the MSL for the contrast between the main lobe and the residual image (d). At last, the mid-range trade-off outperforms both regular and spiral distributions in both FWHM and MSL measurement.

By looking at the VS distribution for the optimized solutions, the VS are distributed close to the maximum elevation angle, approaching the maximum possible aperture, for a better lateral resolution while they gather closer to the center, reducing the inter-VS space for a lower secondary lobe effect, as mentioned in [9]. The mid-range optimized distribution appears as a mixture of positions optimized for either the MSL and the FWHM.

IV. Conclusion

This study shows that image quality can be improved by using optimized distribution of virtual sources instead of regular distribution, which is often used in practice when applying coherent compounding with diverging waves. A drop of 4.4 dB for main-to-side-lobe level and 0.27 mm for lateral resolution is achieved on a 3D point spread function for a distribution optimized for the two quality metrics (full width at half maximum and main-to-side-lobe level), in comparison with a regular distribution. The optimized distribution can be adapted according to the application, and the optimization framework can take into account other imaging algorithms, such as a correlation-based algorithm [18]. However, as this optimization is conducted within the framework of a single scatterer, the emphasis is put on the scatterer's location, notwithstanding the other directions, so that the image quality will be non-homogeneous. This optimization framework is currently being extended to more complex medium, like many scatterers located at different depth, lateral and elevation positions, or a more sophisticated medium as a cyst phantom, in order to be more realistic.

Acknowledgment

This work was supported by the Region Auvergne Rhone Alpes within the program SCUSI in France, by the LABEX CELYA (ANR-10-LABX-0060) of Université de Lyon in France, by the LABEX PRIMES (ANR-11-LABX-0063) of Univesité de Lyon in France and by the Natural Sciences and Engineering Research Council (NSERC) in Canada.

References

[1] G. Stetten, T. Ota, C. Ohazama, C. Fleishman, J. Castelucci, J. Oxaal, T. Ryan, J. Kisslo, and O. Ramm, "Real-time 3D ultrasound: A new look at the heart," vol. 15, 01 1998.

[2] J. Provost, C. Papadacci, J. E. Arango, M. Imbault, M. Fink, J.-L. Gennisson, M. Tanter, and M. Pernot, "3D ultrafast ultrasound imaging *in vivo*," *Physics in Medicine and Biology*, vol. 59, no. 19, pp. L1–L13, Oct. 2014.

[3] G. Montaldo, M. Tanter, J. Bercoff, N. Benech, and M. Fink, "Coherent plane-wave compounding for very high frame rate ultrasonography and transient elastography," *IEEE Transactions on Ultrasonics, Ferroelectrics, and Frequency Control*, vol. 56, no. 3, pp. 489–506, Mar. 2009.

[4] J. Jensen and N. Svendsen, "Calculation of pressure fields from arbitrarily shaped, apodized, and excited ultrasound transducers," *IEEE Transactions on Ultrasonics, Ferroelectrics and Frequency Control*, vol. 39, no. 2, pp. 262–267, Mar. 1992. [Online]. Available: http://ieeexplore.ieee.org/document/139123/

[5] J. Jensen, "Field: A program for simulating ultrasound systems," *Medical and Biological Engineering and Computing*, vol. 34, pp. 351–352, 01 1996.

[6] *MATLAB and Optimization Toolbox version 9.4.0.813654 (R2018a)*. Natick, Massachusetts: The MathWorks Inc., 2018.

[7] P. Mattesini, G. Le Moign, E. Roux, E. Badescu, L. Petrusca, O. Bassett, P. Tortoli, and H. Liebgott, "Optimal Virtual Sources Distribution in 3-D Diverging Wave Ultrasound Imaging: An Experimental Study," in *2018 IEEE International Ultrasonics Symposium (IUS)*. Kobe: IEEE, Oct. 2018, pp. 1–4. [Online]. Available: https://ieeexplore.ieee.org/document/8579668/

[8] P. Sam, "https://fr.mathworks.com/matlabcentral/fileexchange/17997-minimamaxima3d," 2019-08-19.

[9] C. Papadacci, "Imagerie échographique ultrarapide du cœur et des artères chez l'homme: Vers l'imagerie ultrarapide 3D et l'imagerie du tenseur de rétrodiffusion ultrasonore," Ph.D. dissertation, Université Paris VII – Denis Diderot, 2014.

[10] K. Deb, "Multi-Objective Optimization Using Evolutionary Algorithms: An Introduction," p. 25.

[11] M. Ehrgott, *Multicriteria optimization*, 2nd ed. Berlin ; New York: Springer, 2005.

[12] C. A. C. Coello, G. B. Lamont, and D. A. V. Veldhuizen, *Evolutionary Algorithms for Solving Multi-Objective Problems Second Edition*.

[13] C. Darwin, *On the origin of species, 1859*. Routledge, 2004.

[14] J. H. Holland, *Adaptation in natural and artificial systems: An introductory analysis with applications to biology, control, and artificial intelligence.*, ser. Adaptation in natural and artificial systems: An introductory analysis with applications to biology, control, and artificial intelligence. Oxford, England: U Michigan Press, 1975.

[15] J. Kennedy and R. Eberhart, "Particle Swarm Optimization," p. 7, 1995.

[16] K. Deb, S. Agrawal, A. Pratap, and T. Meyarivan, "A Fast Elitist Non-dominated Sorting Genetic Algorithm for Multi-objective Optimization: NSGA-II," in *Parallel Problem Solving from Nature PPSN VI*. Berlin, Heidelberg: Springer Berlin Heidelberg, 2000, vol. 1917, pp. 849–858.

[17] E. Roux, F. Varray, L. Petrusca, C. Cachard, P. Tortoli, and H. Liebgott, "Experimental 3-D Ultrasound Imaging with 2-D Sparse Arrays using Focused and Diverging Waves," *Scientific Reports*, vol. 8, no. 1, Dec. 2018. [Online]. Available: http://www.nature.com/articles/s41598-018-27490-2

[18] N. Quaegebeur and P. Masson, "Correlation-based imaging technique using ultrasonic transmit–receive array for Non-Destructive Evaluation," *Ultrasonics*, vol. 52, no. 8, pp. 1056–1064, Dec. 2012. [Online]. Available: http://www.sciencedirect.com/science/article/pii/S0041624X12001709